NeuroImage: Clinical 7 (2015) 605–610

Contents lists available at ScienceDirect

NeuroImage: Clinical

journal homepage: www.elsevier.com/locate/ynicl

The feasibility of white matter volume reduction analysis using SPM8 plus DARTEL for the diagnosis of patients with clinically diagnosed corticobasal syndrome and Richardson's syndrome

Keita Sakurai[a,*], Etsuko Imabayashi[a], Aya M. Tokumaru[a], Shin Hasebe[a], Shigeo Murayama[b], Satoru Morimoto[b], Kazutomi Kanemaru[b], Masaki Takao[c], Yuta Shibamoto[d], Noriyuki Matsukawa[e]

[a]Department of Diagnostic Radiology, Tokyo Metropolitan Medical Center of Gerontology
[b]Department of Neurology, Tokyo Metropolitan Geriatric Hospital
[c]Department of Neuropathology (the Brain Bank for Aging Research), Tokyo Metropolitan Geriatric Hospital, Tokyo Metropolitan Geriatric Hospital and Institute of Gerontology
[d]Department of Radiology, Nagoya City University Graduate School of Medical Sciences
[e]Department of Neurology and Neuroscience, Nagoya City University Graduate School of Medical Sciences

ARTICLE INFO

Article history:
Received 20 November 2013
Received in revised form 17 February 2014
Accepted 19 February 2014
Available online 27 February 2014

Keywords:
Corticobasal degeneration (CBD)
Progressive supranuclear palsy (PSP)
Statistical parametric mapping (SPM)
Diffeomorphic anatomical registration through exponentiated lie algebra (DARTEL)
Voxel-based specific regional analysis system for Alzheimer's disease (VSRAD)

ABSTRACT

Purpose: Diagnosing corticobasal degeneration (CBD) and progressive supranuclear palsy (PSP) is often difficult due to the wide variety of symptoms and overlaps in the similar clinical courses and neurological findings. The purpose of this study was to evaluate the utility of white matter (WM) atrophy for the diagnosis of patients with clinically diagnosed CBD (corticobasal syndrome, CBS) and PSP (Richardson's syndrome, RS).
Methods: We randomly divided the 3D T1-weighted MR images of 18 CBS patients, 33 RS patients, and 32 age-matched controls into two groups. We obtained segmented WM images in the first group using Voxel-based specific regional analysis system for Alzheimer's disease (VSRAD) based on statistical parametric mapping (SPM) 8 plus diffeomorphic anatomical registration through exponentiated Lie algebra. A target volume of interest (VOI) for disease-specific atrophy was subsequently determined in this group using SPM8 group analyses of WM atrophy between patients groups and controls. We then evaluated the utility of these VOIs for diagnosing CBS and RS patients in the second group. *Z* score values in these VOIs were used as the determinant in receiver operating characteristic (ROC) analyses.
Results: Specific target VOIs were determined in the bilateral frontal subcortical WM for CBS and in the midbrain tegmentum for RS. In ROC analyses, the target VOIs of CBS and RS compared to those of controls exhibited an area under curve (AUC) of 0.99 and 0.84, respectively, which indicated an adequate diagnostic power. The VOI of CBS revealed a higher AUC than that of RS for differentiating between CBS and RS (AUC, 0.75 vs 0.53).
Conclusions: Bilateral frontal WM volume reduction demonstrated a higher power for differentiating CBS from RS. This VOI analysis is useful for clinically diagnosing CBS and RS.

1. Introduction

Corticobasal degeneration (CBD) is a slowly progressive neurodegenerative disorder characterized by tau pathology and distinctive clinical manifestations including asymmetric akinetic-rigid syndrome and higher cortical dysfunctions such as ideomotor apraxia, cortical sensor loss, and alien limb (Lang, et al., 1994; Litvan et al., 2003; Boeve et al., 2003). Clinical features related to dysfunctions in the basal ganglia are also present in patients with progressive supranuclear palsy (PSP), but are generally symmetric and associated with impairment of infratentorial structures (vertical gaze palsy and early falls) (Litvan et al., 1996). Apart from such differences in clinical presentation, an overlap in symptoms has been reported between CBD and PSP, which makes a differential diagnosis between these neurodegenerative disorders challenging (Boeve et al., 2003; Scaravilli et al., 2005). Moreover, the classic neuropathology of CBD is found in patients who presented with progressive aphasia or frontotemporal dementia, making it difficult to maintain the term CBD as a unified clinicopathological entity. The evidence of this poor clinicopathological correlation has led to the use of the term corticobasal syndrome (CBS) in clinically diagnosed CBD cases (Kertesz et al., 2000).

* Correspondence to: to Keita Sakurai, M.D., Department of Diagnostic Radiology, Tokyo Metropolitan Medical Center of Gerontology, 35-2 Sakaecho, Itabashi-ku, Tokyo 173-0015, Japan, Tel: +81-3-3964-1141 Fax: +81-3-3964-1982.
E-mail address: ksak666@yahoo.co.jp (K. Sakurai).

http://dx.doi.org/10.1016/j.nicl.2014.02.009

In addition to characteristic clinical symptoms, previous magnetic resonance imaging (MRI) studies have reported distinct neuroimaging findings of clinically or pathologically diagnosed CBD (CBS/CBD), including asymmetric atrophy in the cerebral cortex and peduncle with dominance contralateral to the more clinically affected side, atrophy of the midbrain tegmentum and corpus callosum, and abnormal T2 prolongation in the subcortical white matter (WM) (Yamauchi et al., 1998; Tokumaru et al., 2009; Koyama et al., 2007). Nevertheless, the diagnostic accuracy of MRI abnormalities is suboptimal for clinically diagnosed PSP (sensitivity averaging approximately 70% across different studies) and poor for CBD (Schrag et al., 2000; Yekhlef et al., 2003; Righini et al., 2004; Gröschel et al., 2006; Josephs et al., 2004). These disorders can also have similar structural abnormalities including atrophy of the midbrain tegmentum and asymmetric atrophy of the cerebral cortex (Tokumaru et al., 2009; Koyama et al., 2007; Boeve et al., 1999).

Voxel-based morphometry (VBM), which can objectively assess the whole brain structure with voxel-by-voxel comparisons, has been developed to analyze tissue volumes between subject groups to distinguish degenerative diseases with Parkinsonism. Previous VBM studies comparing cerebral atrophy between CBS/CBD and PSP patients confirmed more asymmetric dorsal frontal and parietal gray matter (GM) atrophy in CBS/CBD, and more midbrain tegmental atrophy in PSP (Boxer et al., 2006; Josephs et al., 2008). In addition to these findings, subcortical frontal WM atrophy, which may reflect primary degeneration due to tauopathy, has been reported using mainly the SPM 2 and 5 (Boxer et al., 2006; Josephs et al., 2008). However, data on the utility of WM atrophy for differentiating between clinically diagnosed CBD and PSP using the SPM8 plus diffeomorphic anatomical registration through exponentiated Lie algebra (DARTEL) (Wellcome Trust Centre for Neuroimaging, London, UK) method (Ashburner, 2007), which can improve registration and provide the precise location of structural damage in both GM and WM, are scant. The aim of this study was to compare the utility of structural WM atrophy evaluated using SPM8 plus DARTEL for differentiating between patients with a clinical diagnosis of CBD—reported here as CBS—and patients with the classic clinical phenotype of PSP—reported here as Richardson's syndrome (RS).

2. Materials and methods

2.1. Patients and control subjects

The aim of this study was to evaluate the characteristic WM atrophy of CBS and RS using data retrospectively collected at a single medical center. This study was approved by the Ethics Committee for Clinical Research of the Tokyo Metropolitan Medical Center of Gerontology, which waived the requirement for informed consent. The privacy of the patients was completely protected. In this retrospective study, the study group was selected following a search of the medical records filed at the Tokyo Metropolitan Medical Center of Gerontology between March 2007 and March 2013. Patient backgrounds were standardized by applying the following inclusion criteria: (1) clinical diagnoses according to the published criteria of CBS and PSP (Lang et al., 1994; Litvan et al., 1996), and (2) acquisition of 3D T1-weighted SPGR images. An exclusion criterion was the insufficient quality of 3D T1-weighted SPGR images due to significant abnormal findings (e.g., large cerebral infarctions) and apparent artifacts which disturb the VBM analyses. During this period, a total of 59 patients were suspected to have CBS or PSP. Of these, eight patients were excluded due to insufficient MRI qualities. Eighteen CBS (mean age, 79 ± 5 years; 3 men and 15 women) and 33 RS (4 possible and 29 probable) (mean age, 78 ± 5 years; 20 men and 13 women) patients were finally enrolled in this study. Patient characteristics were summarized in Table 1. Thirty-two age-matched people (mean age, 79 ± 3 years; 19 men and 13 women) without obvious neurological or MR abnormalities were selected from the normal database of the volunteer subjects at our institution, and were investigated as control subjects.

2.2. MRI protocol

All 83 patients underwent MRI examinations on a 1.5-T imager (Signa Excite HD; GE Medical systems, Milwaukee, WI, USA) with a multichannel head coil. 3D sections of T1-weighted spoiled gradient recalled echo sequence (SPGR) were mainly obtained in a sagittal plane, for which the scanning parameters were as follows: repetition time 21 ms; echo time 6 ms; flip angle 20°; field of view 230 mm; matrix, 256 × 192 (i.e., in-plane resolution 0.90 × 1.20 mm); and 1.8-mm thick gapless sections. 3D SPGR of four CBS patients were obtained in the axial plane with the same in-plane resolution. All volumetric T1-weighted images were visually inspected for apparent artifacts due to patient motion or metallic dental prostheses.

2.3. Image analysis

Using the software program, VSRAD based on SPM8 plus DARTEL (Matsuda et al., 2012), SPGR images of all subjects were classified into GM, WM, and cerebrospinal fluid images using a unified tissue-segmentation procedure after image-intensity nonuniformity correction, anatomically standardized to a customized template of WM using DARTEL, and were then smoothed using an 8-mm full width at half maximum isotropic Gaussian kernel. VSRAD provided statistical *Z* score images for WM atrophy in each of the patients relative to that of the "normal" database of WM (Nakatsuka et al., 2013). The *Z* score was defined as: ([control mean] − [individual value]) / (control SD).

In order to confirm the diagnostic accuracy (Nakatsuka et al., 2013), we divided 18 patients with CBS, 33 patients with RS, and 32 controls into two groups at random; Group A consisted of 9 CBS patients, 17 RS patients, and 16 controls, and Group B consisted of 9 CBS patients, 16 RS patients, and 16 controls. The WM reduction pattern of CBS and RS patients compared to the others in group A was then assessed by segmented WM images on SPM8 full-factorial analysis. The statistical threshold was set at $p < 0.001$ uncorrected for multiple comparisons with an extent threshold of 300 voxels. Age and sex were included in the model as covariates.

The target volumes of interest (VOI) specific for CBS and RS were then determined using the results of group A analyses. We evaluated the usefulness of these target VOIs for diagnosing the remaining 9 CBS patients and 16 RS patients in group B. We obtained averaged positive *Z* scores in the target VOIs with MRIcron (http://www.mccauslandcenter.sc.edu/mricro/mricron/). Using these averaged positive *Z* scores in the target VOI as a threshold, we used IBM SPSS statistics 21 (IBM SPSS Inc, Chicago, IL, USA) to determine receiver operating characteristic (ROC) curves for discriminating CBS and RS patients.

2.4. Statistical analysis

Statistical analysis was carried out using IBM SPSS statistics 21. A one-way ANOVA, the Kruskal–Wallis test, the unpaired *t* test, Chi-square test and the Mann–Whitney *U* test were used to assess differences in patient characteristics between the groups. Pearson product-moment and Spearman's rank correlation coefficient were used to assess the correlation between the degree of WM atrophy and clinical parameters including the disease duration and Hoehn-Yahr stage at time of MRI scan. Differences were considered significant when $p < 0.05$.

3. Results

Patient characteristics have been summarized in Table 1. No significant difference was observed in age among the CBS, RS, and control

Table 1
Patient and control characteristics.

	CBS (n = 18)	RS (n = 33)	Control (n = 32)	*p* value
Age at the time of MRI (y)	79 ± 5	78 ± 6	79 ± 3	0.67 *
Age at symptom onset (y)	74 ± 5	74 ± 5	NA	0.43 **
Male/Female	3/15	20/13	19/13	0.005 ***
Disease duration at time of MRI (y)	4.6 ± 2.3 (1-9)	4.8 ± 2.6 (1-10)	NA	0.79 **
Neurological examination findings at the time of MRI				
Asymmetry	18 (100%)	4 (12%)	NA	<0.001 ****
Tremor	6 (33%)	8 (24%)	NA	0.49 ****
Rigidity	18 (100%)	32 (97%)	NA	0.46 ****
Limb apraxia	14 (78%)	1 (3%)	NA	<0.001 ****
Apraxia of speech	12 (67%)	2 (6%)	NA	<0.001 ****
Alien limb	2 (13%) [a]	1 (3%)	NA	0.19 ****
Myoclonus	4 (25%) [a]	0 (0%)	NA	0.003 ****
vertical gaze limitation	5 (28%)	25 (76%)	NA	<0.001 ****
Falls	9 (64%) [b]	33 (100%)	NA	<0.001 ****
L-dopa benefit (subjective)	0 (0%)	7 (21%)	NA	0.04 ****
Yahr stage	3.8 ± 1.0	3.9 ± 0.9	NA	0.68 *****
1	0	1	NA	
2	0	2	NA	
2.5	3	2	NA	
3	2	6	NA	
4	8	14	NA	
5	5	8	NA	

Data are shown as absolute numbers or the mean ± standard deviation
Note — CBS = corticobasal syndrome, NA = not applicable, RS = Richardson's syndrome, y = years
* One-way ANOVA
** The unpaired *t* test
*** Kruskal–Wallis test
**** Chi-square test
***** Mann–Whitney *U* test
[a] There were no relevant data in the medical records of two CBS patients
[b] There were no relevant data in the medical records of four CBS patients

groups. No significant difference was also identified in the Hoehn and Yahr scale between the CBS and RS groups. The number of women was markedly higher than that of men in the CBS group; however, this was not observed in the RS or control groups. In the 18 CBS patients, symptoms were right dominant in 12 and left dominant in six.

On full-factorial analysis, widespread patterns of WM reduction were mainly identified in the bilateral frontal and limbic subcortical WM and midbrain (Fig. 1). Patterns of WM reduction in each of the CBS and RS groups compared to the others are shown in Table 2. The most significant areas of atrophy observed in CBS patients compared to the controls were the bilateral frontal subcortical WM including the left precentral gyrus (Fig. 2A, Table 2). The most significant areas of atrophy observed in RS patients compared to the controls were in the midbrain (Fig. 2B, Table 2). Additionally, the atrophy of the corpus callosum in the CBS groups, and subcortical frontal WM in the PSP groups were observed at a more lenient threshold of $P < 0.05$. More atrophic lesions were found in CBS patients than in RS patients, especially in the bilateral cingulate and right postcentral gyrus (Fig. 3A, Table 2). On the other hand, significant atrophy was identified in the bilateral midbrain in RS patients (Fig. 3B, Table 2).

The target VOIs of CBS- and RS-specific atrophy were determined from the results of VBM analyses (Fig. 4A, B). ROC analyses using the averaged positive *Z* scores of CBS, RS, and control subjects were performed to evaluate the diagnostic accuracy of disease-specific VOIs (Fig. 5A–D). A target VOI of CBS including the bilateral frontal subcortical WM exhibited an area under curve (AUC) of 0.99, sensitivity of 89%, specificity of 100%, and accuracy of 96% with a cutoff *Z*-score of 1.30 (Fig. 5A). A target VOI of RS including the midbrain exhibited an AUC of 0.84, sensitivity of 81%, specificity of 81%, and accuracy of 81% with a cutoff *Z*-score of 0.97 (Fig. 5B). These results indicated the adequate discrimination power of disease-specific VOIs to differentiate CBS and RS patients from normal controls. On the other hand, a comparison of the averaged positive *Z* scores to differentiate CBS from RS patients revealed the higher discrimination power of CBS-specific VOI than that of RS-specific VOI (AUC of 0.75 for CBS-specific VOI vs AUC of 0.53 for RS-specific VOI) (Fig. 5C, D). These results indicated that CBS-specific VOI in the bilateral frontal WM could diagnose 89% of CBS patients and exclude 63% of RS patients from the patient group (i.e., sensitivity 89%, specificity 63% with a cutoff *Z*-score of 1.37). Although RS-specific VOI in the midbrain diagnosed 88% of PSP patients, this VOI could not exclude 56% of CBS patients (i.e., sensitivity 88%, specificity 44% with a cutoff *Z*-score of 0.83).

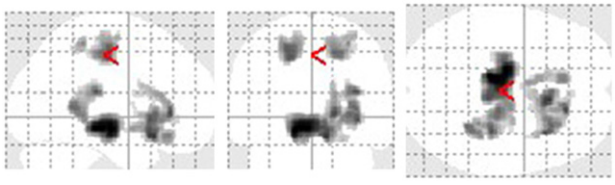

Fig. 1. Regions of WM reduction identified on full-factorial analysis among CBS patients, RS patients, and controls. Widespread patterns of WM reduction are mainly identified in the bilateral frontal and limbic subcortical WM and midbrain. The most significant areas of atrophy within the frontal and limbic lobes include the left anterior cingulate and right medial frontal gyrus. The SPM of the f statistics is displayed in a standard format as a maximum intensity projection viewed from the right-hand side (left image), the back (middle image), and the top (right image) of the brain.

CBS patients revealed a moderately positive correlation between WM atrophy (i.e., *Z*-score in the VOI) and Hoehn-Yahr stage ($r = 0.5$, $P = 0.035$). On the other hand, this correlation was weak in RS patients ($r = 0.3$, $P = 0.07$). There were no correlations between WM atrophy and disease duration at the time of MRI scan in these patients ($r = 0.09$, $P = 0.73$ in CBS and $r = 0.02$, $P = 0.9$ in RS patients).

Table 2.
Comparisons of CBS, RS and NC groups showing the locations in which WM reductions were greater in one group than in the other.

	Region volume (cluster)	t−value	Talairach coordinates (x, y, z)	Location of local maxima
NC > CBS	973	5.76	−20, −15, 46	left precentral gyrus
	1210	5.69	18, −19, 44	right cingulate gyrus
		4.81	33, −18, 56	right precentral gyrus
		4.57	10, 3, 54	right middle frontal gyrus
NC > RS	2132	6.91	−13, −17, −6	left midbrain
		5.21	15, −15, −6	right midbrain
RS > CBS	939	5.27	−18, −18, 42	left cingulate gyrus
		4.36	−14, −16, 56	left medial frontal gyrus
	911	5.05	29, −36, 51	right postcentral gyrus
		4.85	22, −23, 44	right cingulate gyrus
		4.59	27, −8, 55	right middle frontal gyrus
CBS > RS	932	4.87	6, −33, −4	right midbrain
		4.82	−9, −31, −6	left midbrain

Clusters of WM SPM analysis uncorrected at $p < 0.001$ with an extent threshold of 300 voxels are shown. The coordinates refer to the Talairach reference space.
Note − CBS = corticobasal syndrome, NC = normal controls, RS = Richardson's syndrome

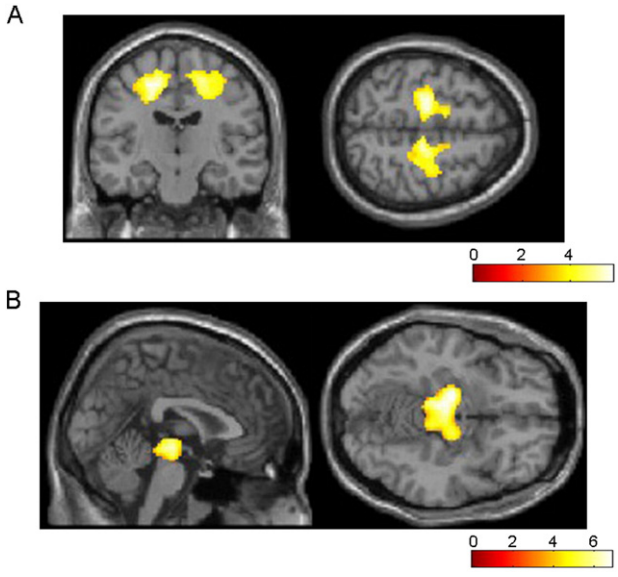

Fig. 2. Regions of WM reduction in CBS (A) and RS (B) patients relative to controls. The most significant areas of atrophy observed in 9 CBS patients compared to 16 controls are the bilateral frontal subcortical WM including the left dominant bilateral precentral and right cingulate gyrus (A). The most significant areas of atrophy observed in 17 RS patients compared to 16 controls are in the bilateral midbrain (B). Significance maps of WM reduction in CBS and RS patients are superimposed on a T1-weighted brain MRI template image in the Montreal Neurological Institute space. The color bar represents the *t* value.

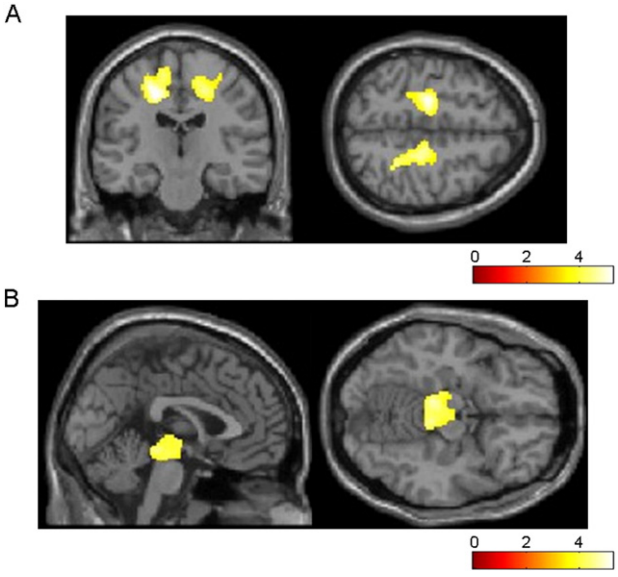

Fig. 3. Regions of WM reduction in CBS (A) and RS (B) patients relative to the others. More atrophic lesions are found in 9 CBS patients than in 17 RS patients, especially in the bilateral cingulate, right postcentral, and right middle frontal gyrus (A). On the other hand, significant atrophy is observed in the bilateral midbrain in RS patients (B). Significance maps of WM reduction in CBS and RS patients are superimposed on a T1-weighted brain MRI template image in the Montreal Neurological Institute space. The color bar represents the *t* value.

4. Discussion

To the best of our knowledge, this is the first study to focus on the diagnostic value of WM volume reduction for discriminating between clinically diagnosed CBD (i.e., CBS) and PSP (i.e., RS) patients by VBM using SPM8 plus DARTEL. The present study demonstrated CBS-specific left-side dominant asymmetric atrophy in the bilateral frontal subcortical WM around the precentral gyrus. This asymmetric nature resulted from the asymmetric symptoms of CBS patients in this study. The WM abnormality of CBS was consistent with previously reported neuroradiological and pathological findings in CBS/CBD (Tokumaru et al., 2009; Koyama et al., 2007; Doi et al., 1999). Conventional MRI studies previously revealed asymmetric cerebral atrophy and subcortical WM T2 prolongation, especially around the central sulcus, with greater prominence contralateral to the more severely affected side (Tokumaru et al., 2009; Koyama et al., 2007; Doi et al., 1999). Additionally, advanced techniques including diffusion-weighted and diffusion tensor imaging have also reported the microstructural abnormalities of cerebral WM including the precentral gyrus, corpus callosum and corticospinal tract (Erbetta et al., 2009; Rizzo et al., 2008; Boelmans et al., 2009). Pathological examinations of WM lesions correlated with the T2 prolongation on MRI have shown the gliosis, demyelination, and tauopathy associated with CBD (Tokumaru et al., 2009; Doi et al., 1999). A semiquantitative analysis revealed similar pathological findings in the subcortical WM relative to the GM in CBD patients (Ksiezak-Reding et al., 1994).

Previous VBM studies of CBS/CBD patients mainly evaluated GM atrophy and focused on frontal lobe atrophy, especially around the premotor cortex (Boxer et al., 2006; Josephs et al., 2008; Whitwell et al., 2010; Rohrer et al., 2011; Lee et al., 2011; Whitwell et al., 2011). On the other hand, the results of this study are consistent with a few VBM studies, which revealed WM abnormalities including asymmetric frontal subcortical atrophy, especially around the central sulcus, and the less severe involvement of the brainstem in CBD patients (Josephs et al., 2008). However, these studies did not evaluate the diagnostic

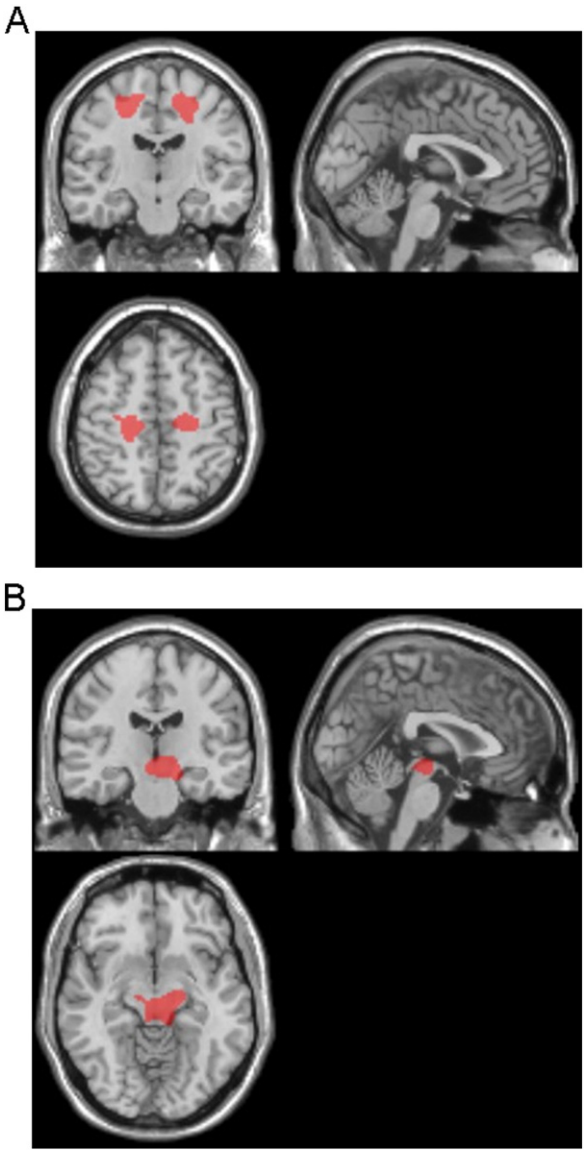

Fig. 4. Target VOIs for CBS- and RS-specific atrophy.The target VOIs of CBS- (A) and RS- (B) specific atrophy are determined from the results of VBM analyses, which reveal the significant bilateral frontal subcortical WM atrophy in CBS patients, and the significant midbrain atrophy in RS patients.

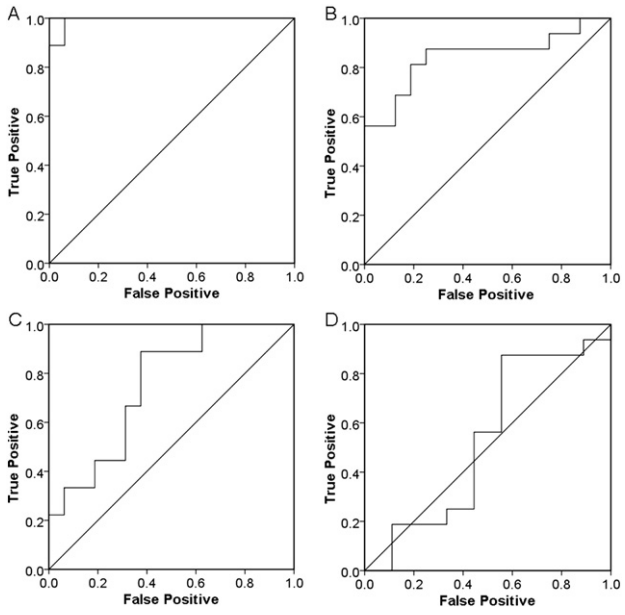

Fig. 5. ROC curves for the diagnosis of CBS (A) and RS (B), and differentiation of CBS from RS by CBS-specific VOI (C) and RS-specific VOI (D) using averaged positive *Z* scores in target VOIs as a threshold.

value of WM atrophy for discriminating between CBS/CBD and RS/PSP. This study demonstrated that the discrimination power of bilateral frontal WM atrophy was higher than that of midbrain tegmental atrophy for differentiating CBS from RS. Considering the pathological data indicating the significantly greater burden of WM abnormalities in CBD than those in PSP (Forman et al., 2002), it is reasonable to evaluate subcortical WM abnormalities when diagnosing CBD and PSP. Abnormal findings of the cingulate gyrus and corpus callosum have also been reported in CBS patients (Yamauchi et al., 1998; Boxer et al., 2006).

If the methodology is only required to discriminate CBS and RS, it is unnecessary to involve control subjects in the procedure for identifying diagnostic VOIs. Indeed, their use may result in a final test with inferior ROC characteristics. However, considering the difficulty in diagnosing parkinsonian syndromes, especially atypical PSP, CBD and multiple system atrophy, it is not always possible for clinicians to narrow down the differential diagnosis only to "PSP" and/or "CBD" on neurological examinations. Thus, we think that it is important to evaluate the diagnostic value of the disease-specific diagnostic VOIs between patients and normal controls, which may support the imaging diagnosis of parkinsonian syndromes.

Midbrain tegmental atrophy is one of the well-known imaging findings of RS/PSP. Not only conventional MRI studies, but also VBM studies have reported the utility of this finding in diagnosing RS/PSP (Boxer et al., 2006; Josephs et al., 2008; Oba et al., 2005; Agosta et al., 2010; Massey et al., 2012). On the surface, the result of the present study revealing the poorer utility of this finding is inconsistent with previous studies. However, some CBS/CBD patients as well as RS/PSP patients can have severe midbrain tegmental atrophy (Tokumaru et al., 2009; Koyama et al., 2007). Clinical symptoms rather than underlying pathology have been shown to have more impact on midbrain tegmental atrophy (Whitwell et al., 2013). Therefore, it is not surprising that the presence of midbrain tegmental atrophy revealed a lower discrimination power.

Furthermore, 3D gradient echo imaging enables not only VBM but also other quantitative evaluations including volume and area measurements, which is useful for diagnosing neurodegenerative diseases (Oba et al., 2005; Quattrone et al., 2008; Shigemoto et al., 2013). Its higher spatial resolution is necessary for the detailed evaluation of various anatomical structures including the midbrain tegmentum, cerebral peduncle, and superior cerebellar peduncle. However, the clinical utility of VOI analyses in this study has not been adequately established, in at least two respects - the group is heterogenous because the scope of the classification is not defined (i.e., severity of symptoms and staging), and no alternative diagnostic tests are considered. Of note is that patients' samples with an unequal size can introduce the bias in VBM analyses and affect the diagnostic value such as accuracy and area under ROC curve (Dubey et al., 2014). Furthermore, our study may have been also limited by the absence of pathological diagnoses in all cases. In this study, CBS patients were diagnosed according to formal diagnostic criteria for research purposes (Litvan et al., 2003). Clinicopathological studies have reported low sensitivity in the ante mortem diagnosis of CBD (Litvan et al., 1997; Ling et al., 2010), and pathological studies have suggested that CBD could present with a broad clinical spectrum including not only CBS, but also non-motor symptoms including disorders of behavior, executive control, and language (Lee et al., 2011; Ling et al., 2010). It is also evident that CBS

is more likely to be caused by various neurodegenerative disorders including PSP (Ling et al., 2010). Despite the very small number of patients, pathologically proven CBD patients revealed different patterns of WM atrophy according to their clinical symptoms (Josephs et al., 2008). Considering the difficulties associated with an ante mortem diagnosis of CBD due to the heterogeneity of clinical symptoms and imaging findings, more pathologically proven cases of CBD are required to reinforce the diagnostic value of WM volume reduction on VBM analysis.

5. Conclusions

Our VBM analysis using SPM8 plus DARTEL demonstrated the diagnostic value of significant atrophy in the bilateral frontal subcortical WM for diagnosing CBS. Thus, the VBM approach can be useful for discriminating between CBS and RS. However, considering the broad clinical spectrum of CBD, more pathologically proven cases of CBD are required to establish the diagnostic value of WM volume reduction on VBM analysis.

Conflicts of interest

This study was supported in part by a Grant-in-Aid for Scientific Research (Kakenhi C) (24,591,785; K.S.).

References

Lang, A., Riley, D.E., Bergeron, C., 1994. Corticobasal ganglionic degeneration. In: DBC (Ed.), Neurodegenerative disease. WB Saunders, Philadelphia, pp. 877–894.
Movement Disorders Society Scientific Issues CommitteeLitvan, I., Bhatia, K.P., Burn, D.J., et al., 2003. Movement Disorders Society Scientific Issues Committee report: SIC Task Force appraisal of clinical diagnostic criteria for parkinsonian disorders. Movement Disorders : Official Journal of the Movement Disorder Society 18, 467–486. http://dx.doi.org/10.1002/mds.1045912722160.
Boeve, B.F., Lang, A.E., Litvan, I., 2003. Corticobasal degeneration and its relationship to progressive supranuclear palsy and frontotemporal dementia. Annals of Neurology 54 (Suppl. 5), S15–S19. http://dx.doi.org/10.1002/ana.1057012833363.
Litvan, I., Agid, Y., Jankovic, J., et al., 1996. Accuracy of clinical criteria for the diagnosis of progressive supranuclear Palsy (Steele–Richardson–Olszewski syndrome). Neurology 46, 922–930. http://dx.doi.org/10.1212/WNL.46.4.9228780065.
Scaravilli, T., Tolosa, E., Ferrer, I., 2005. Progressive supranuclear palsy and corticobasal degeneration: Lumping versus splitting. Movement Disorders 20 (Suppl. 12), S21–S28. http://dx.doi.org/10.1002/mds.2053616092076.
Kertesz, A., Martinez-Lage, P., Davidson, W., et al., 2000. The corticobasal degeneration syndrome overlaps progressive aphasia and frontotemporal dementia. Neurology 55, 1368–1375. http://dx.doi.org/10.1212/WNL.55.9.136811087783.
Yamauchi, H., Fukuyama, H., Nagahama, Y., et al., 1998. Atrophy of the corpus callosum, cortical hypometabolism, and cognitive impairment in corticobasal degeneration. Archives of Neurology 55, 609–614. http://dx.doi.org/10.1001/archneur.55.5.6099605717.
Tokumaru, A.M., Saito, Y., Murayama, S., et al., 2009. Imaging-pathologic correlation in corticobasal degeneration. AJNR. American Journal of Neuroradiology 30, 1884–1892. http://dx.doi.org/10.3174/ajnr.A172119833793.
Koyama, M., Yagishita, A., Nakata, Y., et al., 2007. Imaging of corticobasal degeneration syndrome. Neuroradiology 49, 905–912. http://dx.doi.org/10.1007/s00234-007-0265-617632713.
Schrag, A., Good, C.D., Miszkiel, K., et al., 2000. Differentiation of atypical parkinsonian syndromes with routine MRI. Neurology 54, 697–702. http://dx.doi.org/10.1212/WNL.54.3.69710680806.
Yekhlef, F., Ballan, G., Macia, F., et al., 2003. Routine MRI for the differential diagnosis of Parkinson's disease, MSA, PSP, and CBD. Journal of Neural Transmission 110, 151–169. http://dx.doi.org/10.1007/s00702-002-0785-512589575.
Righini, A., Antonini, A., De Notaris, R., et al., 2004. MR imaging of the superior profile of the midbrain: Differential diagnosis between progressive supranuclear palsy and Parkinson disease. AJNR. American Journal of Neuroradiology 25, 927–93215205125.
Gröschel, K., Kastrup, A., Litvan, I., et al., 2006. Penguins and hummingbirds: Midbrain atrophy in progressive supranuclear palsy. Neurology 66, 949–950. http://dx.doi.org/10.1212/01.wnl.0000203342.77115.bf16567726.
Josephs, K.A., Tang-Wai, D.F., Edland, S.D., et al., 2004. Correlation between antemortem magnetic resonance imaging findings and pathologically confirmed corticobasal degeneration. Archives of Neurology 61, 1881–188415596608.
Boeve, B.F., Maraganore, D.M., Parisi, J.E., et al., 1999. Pathologic heterogeneity in clinically diagnosed corticobasal degeneration. Neurology 53, 795–800. http://dx.doi.org/10.1212/WNL.53.4.79510489043.
Boxer, A.L., Geschwind, M.D., Belfor, N., et al., 2006. Patterns of brain atrophy that differentiate corticobasal degeneration syndrome from progressive supranuclear palsy. Archives of Neurology 63, 81–86. http://dx.doi.org/10.1001/archneur.63.1.8116401739.
Josephs, K.A., Whitwell, J.L., Dickson, D.W., et al., 2008. Voxel-based morphometry in autopsy proven PSP and CBD. Neurobiology of Aging 29, 280–289. http://dx.doi.org/10.1016/j.neurobiolaging.2006.09.01917097770.
Ashburner, J., 2007. A fast diffeomorphic image registration algorithm. NeuroImage 38, 95–113. http://dx.doi.org/10.1016/j.neuroimage.2007.07.00717761438.
Litvan, I., Agid, Y., Calne, D., et al., 1996. Clinical Research Criteria for the Diagnosis of Progressive Supranuclear Palsy (Steele-Richardson-Olszewski syndrome): report of the NINDS-SPSP international workshop. Neurology 47, 1–9.
Matsuda, H., Mizumura, S., Nemoto, K., et al., 2012. Automatic voxel-based morphometry of structural MRI by SPM8 plus diffeomorphic anatomic registration through exponentiated lie algebra improves the diagnosis of probable Alzheimer disease. A.J.N.R. American Journal of Neuroradiology 33, 1109–1114. http://dx.doi.org/10.3174/ajnr.A2935.
Nakatsuka, T., Imabayashi, E., Matsuda, H., et al., 2013. Discrimination of dementia with Lewy bodies from Alzheimer's disease using voxel-based morphometry of white matter by statistical parametric mapping 8 plus diffeomorphic anatomic registration through exponentiated Lie algebra. Neuroradiology 55, 559–566. http://dx.doi.org/10.1007/s00234-013-1138-923322456.
Doi, T., Iwasa, K., Makifuchi, T., et al., 1999. White matter hyperintensities on MRI in a patient with corticobasal degeneration. Acta Neurologica Scandinavica 99, 199–201. http://dx.doi.org/10.1111/j.1600-0404.1999.tb07345.x10100966.
Erbetta, A., Mandelli, M.L., Savoiardo, M., et al., 2009. Diffusion tensor imaging shows different topographic involvement of the thalamus in progressive supranuclear palsy and corticobasal degeneration. AJNR. American Journal of Neuroradiology 30, 1482–1487. http://dx.doi.org/10.3174/ajnr.A161519589886.
Rizzo, G., Martinelli, P., Manners, D., et al., 2008. Diffusion-weighted brain imaging study of patients with clinical diagnosis of corticobasal degeneration, progressive supranuclear palsy and Parkinson's disease. Brain : A Journal of Neurology 131, 2690–2700. http://dx.doi.org/10.1093/brain/awn195 Pubmed: 18819991.
Boelmans, K., Kaufmann, J., Bodammer, N., et al., 2009. Involvement of motor pathways in corticobasal syndrome detected by diffusion tensor tractography. Movement Disorders : Official Journal of the Movement Disorder Society 24, 168–175. http://dx.doi.org/10.1002/mds.2219318973249.
Ksiezak-Reding, H., Morgan, K., Mattiace, L.A., et al., 1994. Ultrastructure and biochemical composition of paired helical filaments in corticobasal degeneration. American Journal of Pathology 145, 1496–15087992852.
Whitwell, J.L., Jack Jr, C.R., Boeve, B.F., et al., 2010. Imaging correlates of pathology in corticobasal syndrome. Neurology 75, 1879–1887. http://dx.doi.org/10.1212/WNL.0b013e3181feb2e821098403.
Rohrer, J.D., Lashley, T., Schott, J.M., et al., 2011. Clinical and neuroanatomical signatures of tissue pathology in frontotemporal lobar degeneration. Brain : A Journal of Neurology 134, 2565–2581. http://dx.doi.org/10.1093/brain/awr19821908872.
Lee, S.E., Rabinovici, G.D., Mayo, M.C., et al., 2011. Clinicopathological correlations in corticobasal degeneration. Annals of Neurology 70, 327–340. http://dx.doi.org/10.1002/ana.2242421823158.
Whitwell, J.L., Jack Jr, C.R., Parisi, J.E., et al., 2011. Imaging signatures of molecular pathology in behavioral variant frontotemporal dementia. Journal of Molecular Neuroscience : MN 45, 372–378. http://dx.doi.org/10.1007/s12031-011-9533-321556732.
Forman, M.S., Zhukareva, V., Bergeron, C., et al., 2002. Signature tau neuropathology in gray and white matter of corticobasal degeneration. American Journal of Pathology 160, 2045–2053. http://dx.doi.org/10.1016/S0002-9440(10)61154-612057909.
Oba, H., Yagishita, A., Terada, H., et al., 2005. New and reliable MRI diagnosis for progressive supranuclear palsy. Neurology 64, 2050–2055. http://dx.doi.org/10.1212/01.WNL.0000165960.04422.D015985570.
Agosta, F., Kostić, V.S., Galantucci, S., et al., 2010. The in vivo distribution of brain tissue loss in Richardson"s syndrome and PSP-parkinsonism: aA VBM-DARTEL study. European Journal of Neuroscience 32, 640–647. http://dx.doi.org/10.1111/j.1460-9568.2010.07304.x20597976.
Massey, L.A., Micallef, C., Paviour, D.C., et al., 2012. Conventional magnetic resonance imaging in confirmed progressive supranuclear palsy and multiple system atrophy. Movement Disorders : Official Journal of the Movement Disorder Society 27, 1754–1762. http://dx.doi.org/10.1002/mds.2496822488922.
Whitwell, J.L., Jack Jr, C.R., Parisi, J.E., et al., 2013. Midbrain atrophy is not a biomarker of progressive supranuclear palsy pathology. European Journal of Neurology 20, 1417–1422. http://dx.doi.org/10.1111/ene.1221223746093.
Quattrone, A., Nicoletti, G., Messina, D., et al., 2008. MR imaging index for differentiation of progressive supranuclear palsy from Parkinson disease and the Parkinson variant of multiple system atrophy. Radiology 246, 214–221. http://dx.doi.org/10.1148/radiol.245306170317991785.
Shigemoto, Y., Matsuda, H., Kamiya, K., et al., 2013. In vivo evaluation of gray and white matter volume loss in the parkinsonian variant of multiple system atrophy using SPM8 plus DARTEL for VBM. NeuroImage: Clinical 2, 491–496. http://dx.doi.org/10.1016/j.nicl.2013.03.017.
Dubey, R., Zhou, J., Wang, Y., et al., 2014. Analysis of sampling techniques for imbalanced data: An n = 648 ADNI study. Neuroimage 87, 220–241. http://dx.doi.org/10.1016/j.neuroimage.2013.10.00524176869.
Litvan, I., Agid, Y., Goetz, C., et al., 1997. Accuracy of the clinical diagnosis of corticobasal degeneration: aA clinicopathologic study. Neurology 48, 119–125. http://dx.doi.org/10.1212/WNL.48.1.1199008506.
Ling, H., O'Sullivan, S.S., Holton, J.L., et al., 2010. Does corticobasal degeneration exist? A clinicopathological re-evaluation. Brain : A Journal of Neurology 133, 2045–2057. http://dx.doi.org/10.1093/brain/awq12320584946.